Available online at www.sciencedirect.com
ScienceDirect
European Polymer Journal 43 (2007) 1916–1922
EUROPEAN POLYMER JOURNAL
www.elsevier.com/locate/europolj

Fluorene-based copolymers for color-stable blue light-emitting diodes

Mingliang Sun, Qiaoli Niu, Renqiang Yang, Bin Du, Ransheng Liu, Wei Yang, Junbiao Peng, Yong Cao *

Institute of Polymer Optoelectronic Materials and Devices, Key Laboratory of Special Functional Materials, South China University of Technology, Guangzhou 510640, People's Republic of China

Received 28 November 2006; received in revised form 27 January 2007; accepted 2 February 2007
Available online 13 February 2007

Abstract

A series of random conjugated copolymers (PFO-HBT) derived from 9,9-dioctylfluorene (DOF) and 2-hexylbenzotriazole (HBT) is prepared by the palladium-catalyzed Suzuki coupling reaction with the feed HBT molar ratio around 1%, 5% and 15%. By copolymerizing 2-hexylbenzotriazole into the backbone of polyfluorene, an efficient colorfast blue light-emitting polymer system is developed. The device with the structure of ITO (indium tin oxide)/PEDOT/PVK/PFO-HBT1/Ba/Al exhibits the highest external quantum efficiency 1.62% with luminance efficiency of 2.69 cd/A, power efficiency of 1.25 lm/W and the CIE coordinates of (0.15, 0.17). The EL spectra are stable at the increased current density and continuous operation without significant change of CIE.

Keywords: Blue emitter; Polymer light emitting device; Polyfluorene; 2-hexylbenzotriazole (HBT); Electroluminescence

1. Introduction

In the last decade, highly-efficiency stable light-emitting conjugated polymers have drawn great attention of researchers for their potential applications both in full-color displays and even in next-generation lighting source, and tremendous progress has been made in this field [1–5]. Of all large band gap light-emitting polymers investigated so far, polyfluorene (PF) and its derivatives have drawn great interests for their exceptional optoelectronic properties, such as good thermal and chemical stability, high fluorescence quantum yield, good film-forming and hole-transporting properties [6–9]. Due to the large energy gap of polyfluorene homopolymer, it is a highly attractive class of conjugated material for applications in polymeric blue light-emitting devices [10,11]. However, PF-based blue light-emitting materials suffer from poor color stability due to the appearance of long-wavelength green emission during continuous device operation or at high current density [12]. This phenomenon is extensively discussed in scientific literatures as a result of the formation of excimer/aggregate

* Corresponding author.
E-mail address: poycao@scut.edu.cn (Y. Cao).

0014-3057/$ - see front matter © 2007 Elsevier Ltd. All rights reserved.
doi:10.1016/j.eurpolymj.2007.02.008

or ketonic defects resulting from photo- and/or electro-oxidation of polyfluorene chains [13–15]. The color stability of polyfluorene can be improved, respectively, by introducing bulky groups to polymer backbone [16], by blending polyfluorene with high glass transition (T_g) temperature material [17] or dielectric nanolayer [18], by introducing a small amount of low bandgap chromophores [19,20] or spirofluorene [21] structure into polyfluorene backbone and by crosslinking the polymers in film states through the end functionalized styryl groups [22].

Recently, Takakazu et al. reported 2-hexylbenzotriazole-based conjugated copolymers with blue photoluminescence [23] and n-type benzotriazole-based conjugated polymers, which are of high photoluminescent quantum yields about 50–70% and electron-accepting property [24].

Due to blue photoluminescence and electron-accepting property of benzotriazole [23,24], in this paper we adopt strategy by introducing a small amount electron acceptor unit (2-hexylbenzotriazole) into the polyfluorene backbone [25] to synthesize an efficient colorfast blue light-emitting polymer system. The best device performance with the structure of ITO (indium tin oxide)/PEDOT/PVK/PFO-HBT1/Ba/Al exhibits the highest external quantum efficiency 1.62% with luminance efficiency of 2.69 cd/A, power efficiency of 1.25 lm/W and the CIE coordinates of (0.15, 0.17).

2. Experimental section

2.1. General methods

^{1}H NMR spectra were recorded on a Bruker DRX 300 spectrometer operating at 300 MHz and was referred to tetramethylsilane. GC-MS were obtained on GC-MS (TRANCE2000, Fiunigan. Co.). Analytical GPC was obtained using a Waters GPC 2410 in tetrahydrofuran (THF) via a calibration curve of polystyrene standards. Elemental analyses were performed on a Vario EL Elemental Analysis Instrument (Elementar Co.). UV–visible absorption spectra were measured on a HP 8453 spectrophotometer. PL spectra in solutions were taken by Fluorolog-3 spectrofluorometer (Jobin-Yvon) under 325 nm light excitation. PL spectra in solid thin films were taken by InstaSpec™ IV CCD spectragraph (Oriel).

Cyclic voltammetry was measured on a Potentiostat/Galvanostat model 283 electrochemical workstation (Princeton Applied Research) at a scan rate of 50 mV/s with a nitrogen-saturated solution of 0.1 M tetrabutylammonium hexafluorophosphate (Bu_4NPF_6) in acetonitrile (CH_3CN), respectively, with platinum and saturated calomel electrodes (SCE) as the working and reference electrodes.

LED was fabricated on pre-patterned indiumtin oxide (ITO) with a sheet resistance 10–20 Ω/□. The substrate was ultrasonically cleaned with acetone, detergent, deionized water and 2-propanol subsequently. Oxygen plasma treatment was made for 10 min as the final step of substrate cleaning to improve the contact angle just before film coating. Onto the ITO glass a 50 nm-thick layer of polyethylenedioxythiophene-polystyrene sulfonic acid (PEDOT:PSS) film was spin-coated from its aqueous dispersion (Baytron P 4083, Bayer AG), aiming at improving the hole injection and avoiding the possibility of leakage. PEDOT:PSS film was dried at 80 °C for 2 h in a vacuum oven. The solution of the PVK in chlorobenzene was prepared in a nitrogen-filled dry box and spin-coated on the top of the ITO/PEDOT:PSS surface. Then the solution of the copolymers (in toluene) was spin-coated on the top of the ITO/PEDOT:PSS PVK surface. The typical thickness of the emitting layer was 70–80 nm. Then a thin layer of barium as an electron injection cathode and the subsequent 200 nm-thick aluminum capping layers were thermally deposited by vacuum evaporation through a mask at a base pressure below 2×10^{-4} Pa. The deposition speed and thickness of the barium and aluminum layers were monitored by a thickness/rate meter (model STM-100, Sycon). The cathode area defines the active area of the device. The typical active area of the devices in this study was 0.17 cm^2. The spin coating of the EL layer and device performance tests were carried out within a glove box (Vacuum Atmosphere Co.) with nitrogen circulation. Current–luminance–voltage (I–L–V) characteristics were measured with a computerized Keithley 236 Source Measure Unit and calibrated Si photodiode. External quantum efficiency was verified by measurement in the integrating sphere (IS080, Lab sphere) and luminance was calibrated by PR705 spectragraph-photometer (Photo Research) after the encapsulation of devices with UV-curing epoxy and thin

cover glass. EL spectra were taken by InstaSpec™ IV CCD spectragraph.

2.2. Materials

All reagents, unless otherwise specified, were obtained from Aldrich, Acros, and TCI Chemical Co., and used as received. All the solvents were further purified under a nitrogen flow. 2,7-Dibromo-9,9-dioctylfluorene (**1**) 2,7-Bis(4,4,5,5-tetramethyl-1,3,2-dioxaborolan-2-yl)-9,9-dioctylfluorene (**2**) [26] 4,7-dibromo-2-hexylbenzotriazole (**3**) [23] were prepared following the procedure described in the reference and characterized by the GC-MS and ^{1}H NMR spectra.

2.3. Synthesis of polymer

Carefully purified 2,7-dibromo-9,9-dioctylfluorene (**1**), 2,7-bis(4,4,5,5-tetramethyl-1,3,2-dioxaborolan-2-yl)-9,9-dioctylfluorene (**2**), 4,7-dibromo-2-hexylbenzotriazole (**3**), $(PPh_3)_4Pd$ (0) (0.5–2.0 mol%) and several drops of Aliquat 336 were dissolved in a mixture of toluene and aqueous 2 M Na_2CO_3. The solution was refluxed with vigorous stirring for 36 h in an argon atmosphere. At the end of polymerization, the polymers were end-capped with 2,7-bis(4,4,5,5-tetramethyl-1,3,2-dioxaborolan-2-yl)-9,9-dioctylfluorene and bromobenzene to remove bromine and boronic ester end groups in order to avoid a possible quenching effect or excimer formation by boronic and bromine end groups in LEDs [27]. The mixture was then poured into methanol and the precipitated material was recovered by filtration and purified by flash column chromatography. The resulted polymers were air-dried overnight, followed by drying in vacuum. In the process of polymerization, the comonomer feed ratios of (**1**+**2**) to **3** were, respectively, 99:1, 95:5 and 85:15, and the mole ratio of 2,7-bis-(4,4,5,5-tetramethyl-1,3,2-dioxaborolan-2-yl)-9,9-dioctylfluorene (**2**) to 2,7-dibromo-9,9-dioctylfluorene (**1**) and 2-hexylbenzotriazole (**3**) was always remained as **2**: (**1**+**3**) = 1:1. The corresponding copolymers were, respectively, named PFO-HBT1, 5, and 15.

2.3.1. PFO-HBT1

2 (0.50 mmol), **1** (0.49 mmol), and **3** (0.01 mmol) were used in this polymerization. yield light-yellow fibers (0.317 g, 81.9% yield). ^{1}H NMR (300 MHz, $CDCl_3$): 7.88–7.86(m), 7.70–7.66(m), 7.39–7.28(m), 2.15(s), 1.28–1.16(m), 0.86–0.82(t, $J = 7.0$).

2.3.2. PFO-HBT5

2 (0.50 mmol), **1** (0.45 mmol), and **3** (0.05 mmol) were used in this polymerization. yield light-yellow fibers (0.285 g, 75.6% yield). ^{1}H NMR (300 MHz, $CDCl_3$): 7.88–7.86(m), 7.70–7.66(m), 7.39–7.28(m), 2.14(s), 1.28–1.16(m), 0.86–0.82(t, $J = 6.9$).

2.3.3. PFO-HBT15

2 (0.50 mmol), **1** (0.35 mmol), and **3** (0.15 mmol) were used in this polymerization. yield light-yellow fibers (0.261 g, 72.4% yield). ^{1}H NMR (300 MHz, $CDCl_3$): 8.09–7.94(m), 7.88–7.86(m), 7.74–7.66(m), 7.39–7.28(m), 4.87–4.81(m), 2.14(s), 1.42(s), 1.28–1.16(m), 0.95–0.82(t, $J = 6.9$).

3. Results and discussion

3.1. Synthesis and chemical characterization

The synthetic routes toward the monomers and copolymers are outlined in Scheme 1. The obtained copolymers are readily soluble in common organic solvents, such as toluene, THF and chloroform. The number-average molecular weights of these polymers are determined by GPC using a polystyrene standard, ranging from 18,000 to 34,500 with a polydispersity index (M_w/M_n) between 1.55 and 1.89 (Table 1). The actual ratios of substituted fluorene (DOF) to low band-gap monomer (HBT) in the copolymers estimated by elemental analysis (N

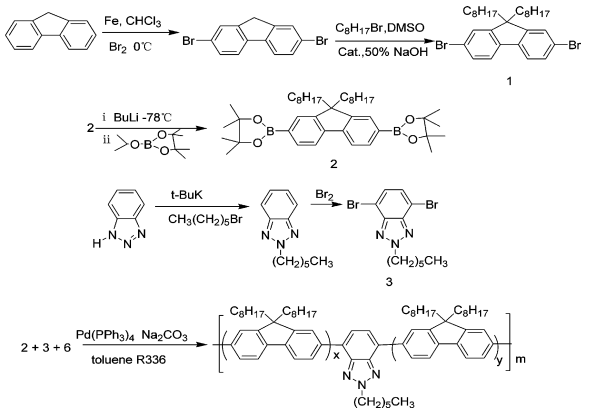

Scheme 1. The synthesis routine of monomers and the copolymers.

Table 1
Molecular weights of the copolymers and their composition determined by elemental analysis

Copolymers	M_n ($\times 10^3$)	M_w/M_n	C content in copolymers (%)	N content in copolymers (%)	The feed ratios of DOF/HBT	DOF/HBT in copolymers[a]
PFO-HBT1	34.5	1.89	88.86	0.20	99:1	98:2
PFO-HBT5	33.5	1.80	88.74	0.38	95:5	96:4
PFO-HBT15	18.0	1.55	87.75	1.23	85:15	86:14

[a] Molar ratio of DOF/HBT in the copolymers calculated from C and N element contents in the copolymers.

and C content) are listed in Table 1, which is in good agreement with the feeding ratios of the two monomers within the experimental error.

3.2. Optical properties and electrochemical characteristics

The UV–vis absorption properties of the conjugated polymers are presented in Table 2. Fig. 1 shows the normalized UV–vis absorption spectra of the polymers in thin solid films and in THF solution. The absorption spectra of copolymers monitored in thin solid films display one absorption band with a small bump near the band edge, the intensity of which increases with increasing HBT content. The absorption spectra of copolymers in THF solution are similar to those of the copolymers in solid films.

The electrochemical properties of the copolymers are investigated by cyclic voltammetry (CV). Table 2 summarizes oxidation potentials derived from the onset of the oxidation wave in the cyclic voltammograms of the copolymers. We can record one p-doping process in all the copolymers, and the onset of oxidation process of these copolymers is around 1.4 V which are attributed to the oxidation process of the DOF segment. The oxidation of HBT unit cannot be detected probably due to low HBT content. The optical band gap (E_g) is estimated from the onset wavelength of UV–vis spectra of the copolymer solid film. HOMO and

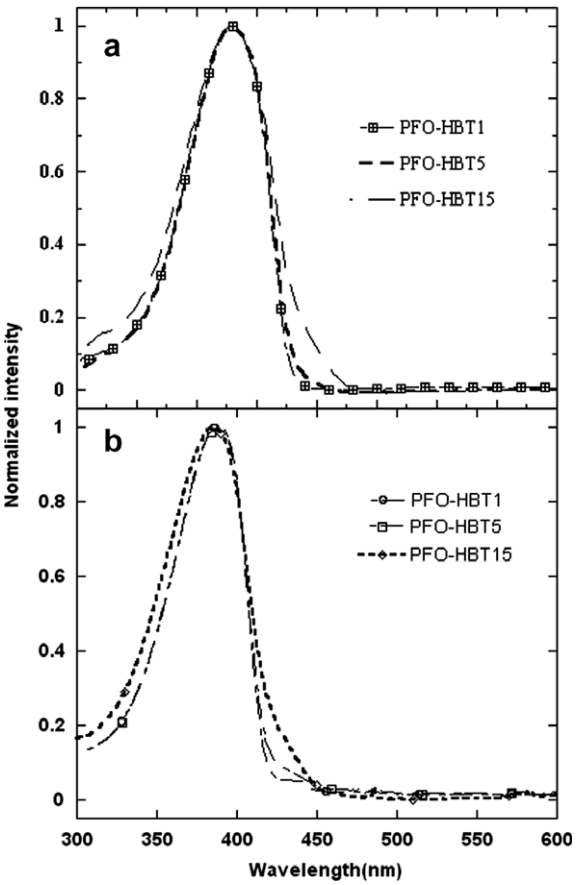

Fig. 1. (a) UV–vis absorption spectra for the copolymers in thin solid films. (b) UV–vis absorption spectra for the copolymers in the THF solution.

Table 2
UV-absorption and electrochemical properties of the copolymers in solid film

Copolymers	$\lambda_{(ABS)max}$ (nm)	Optical band gap[a] (eV)	E_{ox} (V)	HOMO (eV)	LUMO[b] (eV)
PFO-HBT1	382	2.95	1.33	−5.73	−2.78
PFO-HBT5	382	2.93	1.39	−5.79	−2.86
PFO-HBT15	382	2.87	1.40	−5.8	−2.93

[a] Calculated from the onset of the absorption spectra of the copolymers in thin solid films.
[b] Calculated from HOMO and optical band gap of the copolymers, respectively.

LUMO levels calculated by the empirical formulas $E_{HOMO} = -e(E_{ox} + 4.4)$ (eV) and $E_{LUMO} = -e(E_{red} + 4.4)$ (eV) [28] are also listed in Table 2.

3.3. Photoluminescence properties

Fig. 2 shows the normalized PL spectra of the polymers in the solutions of THF at a concentration of $1 * 10^{-3}$ M. The PL emission peaks are 463 nm 462 nm and 468 nm, respectively, for PFO-HBT1, PFO-HBT5 and PFO-HBT15. As shown in Fig. 3, the PL emission in the solid film are red-shifted gradually with increasing the content of HBT in the polymer backbone, peaked at 457, 465 and 472 nm for PFO-HBT1, PFO-HBT5 and PFO-HBT15, respectively. Similar red shift for blue emitting polymers was reported by other group [29] and it could be assigned to increased intermolecular interaction between HBT groups in the neighboring chains in the solid state.

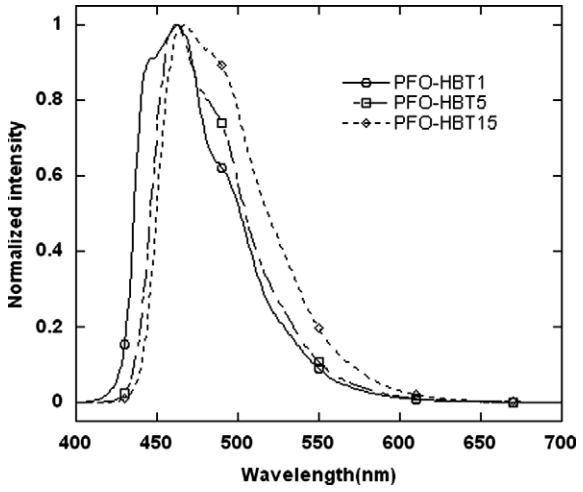

Fig. 2. Normalized PL spectra of the copolymers in THF solution at $1 * 10^{-3}$ mol/L.

3.4. Electroluminescent and J–L–V characteristics of LEDs

Since the HOMO for the copolymer is around 5.7–5.8 eV (Table 2) and the work function of PEDOT is around 5.0–5.2 eV, it would be possible to expect a better hole injection once a PVK (work function 5.5–5.6 eV) is used as the hole injection anode. We fabricate EL devices with a configuration ITO/PEDOT:PSS/PVK/PFO-HBT/Ba/Al. Fig. 4 shows the EL spectra of the copolymers in such devices. The EL emission peaks are 458 nm 464 nm and 470 nm, respectively, for PFO-HBT1, PFO-HBT5, PFO-HBT15. The device ITO (indium tin oxide)/PEDOT/PVK/PFO-HBT1/Ba/Al exhibits the highest external quantum efficiency 1.62% with luminance efficiency of 2.69 cd/A and power efficiency of 1.25 lm/W with the CIE coordinates of (0.15, 0.17). Similar device performance is obtained for PFO-HBT5 copolymer. Table 3 lists device performance for these three copolymers. Similar as PL spectra, EL peaks are red-shifted around 12 nm when HBT content increased from 1% to

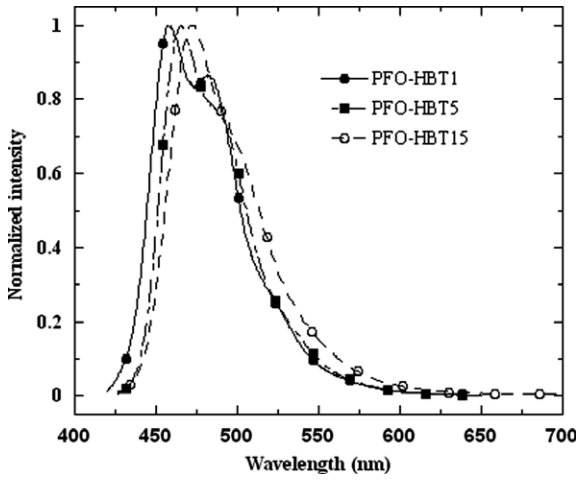

Fig. 3. Normalized PL spectra of the copolymers in thin solid films.

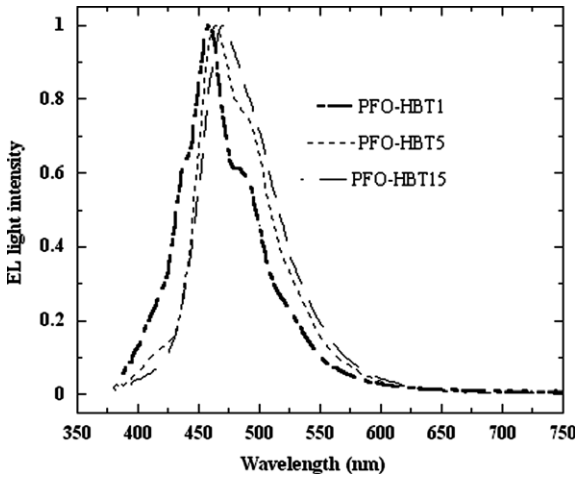

Fig. 4. Normalized EL spectral of the copolymers with device configuration ITO/PEDOT:PSS/PVK/PFO-HBT/Ba/Al.

Table 3
Device performances of the copolymers (ITO/PEDOT:PSS/PVK/polymer/Ba/Al) given at point when devices reached maximum external quantum efficiency

Polymer	λ_{ELmax} (nm)	J (mA/cm^2)	V (v)	L (cd/m^2)	LE (cd/A)	EE (lm/w)	QE_{max} (%)	CIE
PFO-HBT1	458	2.0	6.75	54.3	2.69	1.25	1.62	(0.15, 0.17)
PFO-HBT5	464	13.4	6.5	384	2.87	1.38	1.73	(0.15, 0.24)
PFO-HBT15	470	1.74	6.3	41.9	2.41	1.20	1.45	(0.15, 0.27)

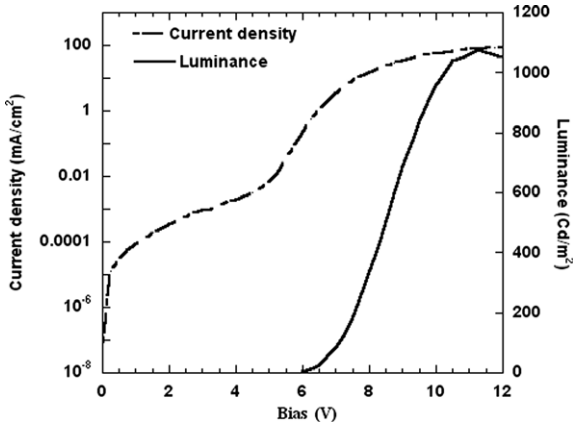

Fig. 5. J–L–V characteristics of LEDs based on PFO-HBT1.

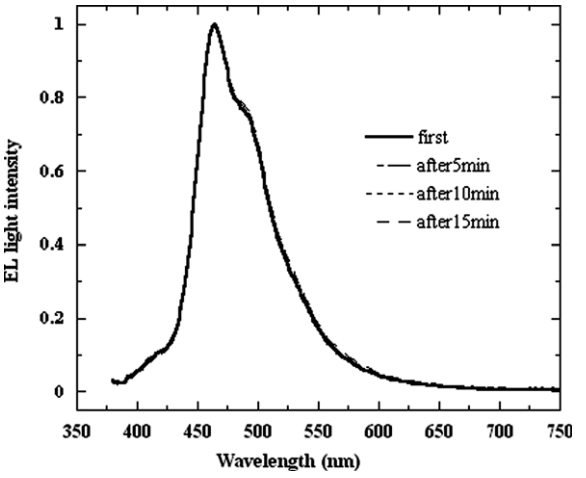

Fig. 7. Normalized EL spectra with device configuration ITO/PEDOT:PSS/PVK/PFO-HBT5/Ba/Al after continuous turn-on at current density of 12 mA/cm^2.

15%. [30] J–L–V curve of the PFO-HBT1-based device is shown in Fig. 5.

We also make preliminary investigation on color stability of PFO-HBT-based device. As shown in Fig. 6, PFO-HBT is found to be good color stability without long wavelength excimer-like emissions at 500–600 nm in wide range of current density. Fig. 7 shows EL spectra of PFO-HBT5-based device taken after 0, 5, 10 and 15 min continuous lighting. Little change in the EL spectra can be observed during the experiment.

4. Conclusions

In summary, we have developed an efficient stable blue emitting fluorene-based copolymer system. The EL spectra are stable at different current density. No undesired long-wavelength green emission is observed in the EL spectra. Devices from the

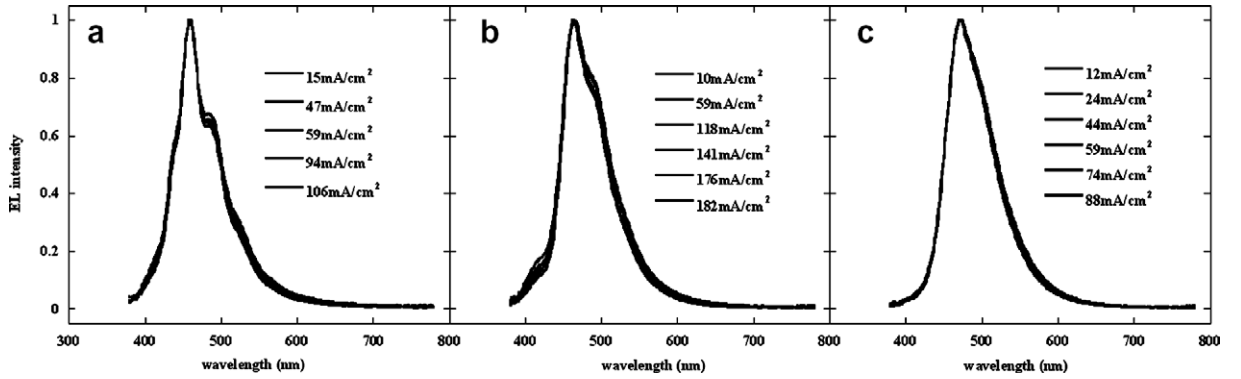

Fig. 6. Normalized EL spectra with device configuration ITO/PEDOT:PSS/PVK/PFO-HBT1 (a) or PFO-HBT1 (b) or PFO-HBT1 (c) Ba/Al at different current density.

resulting copolymers show good color coordinate and color-stability at high current density and in continuous operation.

Acknowledgements

The authors are deeply grateful to the MOST National Research Project (No. 2002CB613405) and the National Natural Science Foundation of China (Project No. 50433030) for financial support.

References

[1] Bernius MT, Inbasekaran M, O'Brien J, Wu W. Adv Mater 2000;12:1737.
[2] Sagar AD, Shingte RD, Wadgaonkar PP, Salunkhe MM. Eur Polym J 2001;37:1493.
[3] Chen B, Wu Y, Wang M, Wang S, Sheng S, Zhu W, Sun R, Tian H. Eur Polym J 2004;40:1183.
[4] Tang RP, Tan ZA, Cheng CX, Li YF, Xi F. Polymer 2005; 46:5341.
[5] Ferreira M, Constantino CJL, Olivati CA, Balogh DT, Aroca RF, Faria RM, et al. Polymer 2005;46:5140.
[6] Kim YH, Shin DC, You H, Kwon SK. Polymer 2005; 46:7969.
[7] Wang F, Luo J, Chen JW, Huang F, Cao Y. Polymer 2005; 46:8422.
[8] Wu WC, Liu CL, Chen WC. Polymer 2006;47:527.
[9] Yang Y, Pei Q, Heeger AJ. J Appl Phys 1996;79:934.
[10] Grice AW, Bradley DDC, Bernius MT, Inbasekaran M, Wu WW, Woo EP. Appl Phys Lett 1998;73:629.
[11] Friend RH, Gymer RW, Holmes AB. Nature 1999;397:121.
[12] Pei QB, Yang Y. J Am Chem Soc 1996;118:7416.
[13] Bliznlyk VN, Carter S, Scott JC, Klärnar G, Miller RD, Miller DC. Macromolecules 1999;32:361.
[14] List EJW, Guentne R, Freitas PS, Scherf U. Adv Mater 2002;14:374.
[15] Kulkarni AP, Kong X, Jenekhe SA. J Phys Chem B 2004;108:8689.
[16] Pogantsch A, Wenzl FP, List EJW, Leising G, Grimsdale AC, Müllen K. Adv Mater 2002;14:1061.
[17] Kulkarni AP, Jenekhe SA. Macromolecules 2003;36:5285.
[18] Park JH, Lim YT, Park OO, Kim JK, Yu JW, Kim YC. Adv Funct Mater 2004;14:377.
[19] Kreyenschmidt M, Klaemer G, Fuhrer T, Ashenhurst J, Karg S, Chen WD, et al. Macromolecules 1998;31:1099.
[20] Klärmer G, Davey MH, Chen WD, Scott JC, Miller RD. Adv Mater 1998;10:993.
[21] Yu WL, Pei J, Huang W, Heeger A. J Adv Mater 2000; 12:828.
[22] Klärmer G, Lee JI, Lee VY, Chan E, Chen JP, Nelson A, et al. Chem Mater 1999;11:1800.
[23] Tanimoto A, Yamamoto T. Adv Synth Catal 2004;346:1818.
[24] Tanimoto A, Yamamoto T. Macromolecules 2006;39:3546.
[25] Kulkarni AP, Zhu X, Jenekhe SA. Macromolecules 2005;38:1553.
[26] Ranger M, Rondeau D, Leclerc M. Macromolecules 1997; 30:7686.
[27] Yang X, Yang W, Yuan M, Hou Q, Huang J, Zeng X, et al. Synth Met 2003;135:189.
[28] Leeuw DM, Simenon MMJ, Brown AR, Einerhand REF. Synth Met 1997;87:53.
[29] Liu XM, He CB, Hao XT, Tan LW, Li YQ, Ong KS. Macromolecules 2004;37:5965.
[30] Hou Q, Zhou Q, Zhang Y, Yang W, Yang RQ, Cao Y. Macromolecules 2004;37:6299.